ECCOMAS Congress 2016
VII European Congress on Computational Methods in Applied Sciences and Engineering
M. Papadrakakis, V. Papadopoulos, G. Stefanou, V. Plevris (eds.)
Crete Island, Greece, 5–10 June 2016

APPROPRIATE COMBINATIONS OF CONTROLLER PARAMETERS FOR UNSTEADY FLOW SIMULATIONS WITH ADAPTIVE TIME STEP CONTROL

Kathrin Kožulović, Graham Ashcroft

Institute of Propulsion Technology, German Aerospace Center (DLR)
Linder Höhe, 51147 Cologne, Germany, http://www.dlr.de/at/
e-mail: kathrin.kozulovic@dlr.de, graham.ashcroft@dlr.de

Keywords: Unsteady Flow, Time Accurate, Runge-Kutta, High Order, Adaptive Time Stepping, Controller Parameter, Error Estimation

Abstract. *Compressible Navier-Stokes equations, which govern unsteady flow phenomena, have been numerically integrated with several high order ESDIRK schemes (Explicit first stage, Stiffly accurate Diagonally Implicit Runge-Kutta). This type of numerical scheme allows for embedded error estimation and, based on this error estimation, for adaptive time stepping, cf. [1, 2, 3]. In this paper different controller types have been applied for the automatic adaption of the time step size to a prescribed accuracy level: I-, PI-, PC- and PID-controller. Depending on the choice of corresponding controller parameters, the simulation time can be varied considerably. On the one hand, a conservative choice leads to slow time step adaption, small step size and long simulation time. On the other hand, an aggressive parameter setting can lead to quick step size adaption, but also to rejected computations, due to large time step size, which does not keep the prescribed accuracy. This also may result in long simulation time. Obviously, there must be appropriate combinations of controller parameters, which minimize the simulation duration. Hence, a systematic study on a large controller parameter space has been conducted and regions with appropriate combinations have been identified. Both generic and complex test cases have been investigated. Overall CPU times and number of time steps are compared among different ESDIRK schemes and controllers. For the generic test case, most schemes show a narrow space for the choice of suitable controller parameters, but only one scheme shows good simulation performance without large sensitivities to parameter combinations. For the complex test cases, all schemes and controllers are less sensitive to parameter combinations. Furthermore, the optimum combination varies strongly with the type of governing equations.*

1 INTRODUCTION

The time integration of unsteady flow simulations can be conducted by different schemes: explicit or implicit, multi-stage or multi-step. In the present work, ESDIRK schemes have been applied, due to their well-balanced combination of favourable features as stability, robustness, embedded error estimation and time step control, cf. [1], [2]. In particular, the ability to adapt the time step size automatically to some prescribed error tolerance is of large benefit for the simulation reliability and efficient use of computational resources. Previous work was focused on implementation and validation of different ESDIRK schemes of 3rd- and 4th-order of accuracy, together with a basic time step control, cf. [4], [5].

Now, the investigation of time step control has been considerably enhanced and the schemes are re-assessed in terms of their computational efficiency. Different time step controllers (I, PI, PID, PC) have been implemented and their parameters have been systematically varied among a very large design space, in order to identify the optimum settings. Two essential mechanisms affect the simulation time. On the one hand, a quick adaption of time step size leads to reduced run time. On the other hand, the simulation time is considerably prolonged if many iterations with rejected error estimates are conducted. The reason therefore is an excessively large time step, usually generated by an overshoot in the automatic time step size controller. In other words, the controller parameters should provide a quick time step size adaption, but prevent the overshoots. As will be shown later, both the type of equation system and of test case require a different controller type with a different combination of corresponding parameters, in order to achieve quick and reliable simulations.

Besides time step controllers, the accuracy order of the applied scheme (for time integration and error estimation) significantly affects the simulation duration. On the one hand, a higher scheme order can lead to larger time steps, hence reducing the runtime. On the other hand, the computational effort per iteration is larger for higher order schemes, which will increase the runtime. These effects, in combination with the aforementioned controller parameters, are the primary influence factors for the simulation duration and will be addressed in the subsequent sections.

2 FLOW SOLVER

The numerical simulations presented in this work are performed using the compressible Navier-Stokes solver TRACE [6], [7]. The TRACE code has been developed at DLR's Institute of Propulsion Technology in Cologne to model and investigate turbomachinery flows. The governing equations are solved using a multi-block approach for both structured and unstructured grids embedded in a parallel environment. The finite-volume method is adopted in generalized coordinates about the cell centers for space discretization. Upwind-biased spatial differencing in conjunction with Roe's flux-difference-splitting method is used to evaluate the inviscid fluxes, with limiters used to obtain smooth solutions in the vicinity of shocks. Viscous terms are discretized using second-order accurate central differences. Turbulence modeling is effected by a $k-\omega$ two-equation approach with turbomachinery-specific extensions. The discretization of the spatial operators in the Navier-Stokes equations results in a system of ordinary differential equations of the following form

$$\frac{d\mathbf{U}}{dt} = \mathbf{R}(t, \mathbf{U}(t)) \tag{1}$$

where $\mathbf{U}$ represents the vector of conservative variables and t denotes the physical time.

3 IMPLICIT RUNGE-KUTTA METHODS

The numerical solution $\mathbf{U}^{n+1}$ of the ordinary differential system 1 at time $t^{n+1} = t^n + \Delta t$ using an s-stage implicit Runge-Kutta scheme is

$$\mathbf{U}^{n+1} = \mathbf{U}^n + \Delta t \sum_{j=0}^{s} b_j \mathbf{R}(t_n + c_j \Delta t, \mathbf{W}^i) \tag{2}$$

with the values of intermediate stages i

$$\mathbf{W}^i = \mathbf{U}^n + \Delta t \sum_{j=0}^{s} a_{ij} \mathbf{R}(t_n + c_j \Delta t, \mathbf{U}^j)\,, \quad i = 1, \ldots, s. \tag{3}$$

The values a_{ij}, b_j and c_j are called Butcher coefficients of the scheme, where the values c_j denote the evaluation time of the intermediate stages in the interval $t_n \rightarrow t_n + \Delta t$ and b_j the contribution of the individual stage to the final solution at the end of the Runge-Kutta step.

3.1 ERROR ESTIMATION

Implicit Runge-Kutta methods allow for error estimation using an embedded method in the same Butcher tableau with different order of accuracy $q = p \pm 1$, with q the order of the scheme advancing the solution and p the order of the error estimation scheme, respectively. The solution $\hat{\mathbf{U}}^{n+1}$ of the embedded scheme is

$$\hat{\mathbf{U}}^{n+1} = \mathbf{U}^n + \Delta t \sum_{j=0}^{s} \hat{b}_j \mathbf{R}(t_n + c_j \Delta t, \mathbf{W}^i), \tag{4}$$

where the values $\hat{b}_j$ are an additional set of solution coefficients appended to the Butcher tableau. The embedded method depends only on linear combinations of already present stage values $\mathbf{W}^i$ which makes the error estimation computationally cheap. The error estimate of embedded IRK methods is defined as

$$\Delta \mathbf{U}^{n+1} = \mathbf{U}^{n+1} - \hat{\mathbf{U}}^{n+1}. \tag{5}$$

Within this investigation the maximum error $||\Delta \mathbf{U}^{n+1}||_\infty = max(|\Delta \mathbf{U}_i^{n+1}|)$ is used.

3.2 ESDIRK SCHEMES

The solution of an n-dimensional differential equation system using an implicit Runge-Kutta method with s stages needs the evaluation of $n \cdot s$ non-linear equation sets per time step. Therefore several simplifications are useful for the successful implementation of these methods.

For diagonally implicit schemes the coefficient matrix a_{ij} is characterized by a lower triangular form, each stage of the scheme therefore depends only on previously solved stages and the system may thus be solved in s successive steps. An additional simplification for this type of scheme is the use of the same diagonal coefficient γ for each stage. For methods with explicit first stage ($a_{1j} = 0$) the stages are at least second-order accurate. The conditions for stiffly accurate methods are $a_{ij} = b_j, j = 1, \ldots, s$, which ensures that the solution of the last stage $\mathbf{U}^s$ is the solution at the next time step $\mathbf{U}^{n+1}$. A four stage example of the Butcher tableau for an Explicit first stage, Singly Diagonal Implicit Runge-Kutta (ESDIRK) scheme is given in Table 1.

	$c_1 = 0$	0	0	0	0
	c_2	a_{21}	γ	0	0
	c_3	a_{31}	a_{32}	γ	0
	$c_4 = 1$	b_1	b_2	b_3	γ
order of accuracy	q	b_1	b_2	b_3	γ
order of accuracy	$p \pm 1$	$\hat{b_1}$	$\hat{b_2}$	$\hat{b_3}$	$\hat{b_4}$

Table 1: Generic Butcher tableau of a four-stage embedded ESDIRK scheme

In this paper stiffly accurate embedded ESDIRK pairs from third-order up to fourth-order proposed by Alexander [1], Carpenter et. al. [2] and Kvaerno [3] are considered for the numerical solution of the compressible Navier-Stokes equations. The schemes are here denoted by authors name followed by the order of accuracy of the solution scheme and in brackets the order of the scheme for error prediction, e.g. Ale 3(2). The formula pairs presented by Kvaerno differ a little from the generic form given in Table 1, as the last two successive stages are evaluated at $c_s = c_{s-1} = 1$ and used either to advance the solution or to estimate the error. In that case the additional coefficients $\hat{b}$ are omitted. The Butcher tableaus of the methods used in the present work are given in Table 2- Table 4.

4 STEP SIZE CONTROL ALGORITHMS

The local error of the numerical solution is observed by the embedded ESDIRK scheme. To control the accuracy of the solution by holding the error within the desired tolerance bounds and to adapt the time step size Δt standard controller types are used. For embedded formula pairs with $q = p \pm 1$ time step control can be conducted using I-, PI-, PID- or PC-controllers [2], [8]. The algorithms to select the time step size for the different controllers are given by

$$\Delta t_I^{n+1} = dt_{fac}\, \Delta t^n \left(\frac{TOL}{||\Delta U^{n+1}||_\infty} \right)^{K_I}, \tag{6}$$

$$\Delta t_{PI}^{n+1} = dt_{fac}\, \Delta t^n \left(\frac{TOL}{||\Delta U^{n+1}||_\infty} \right)^{K_I} \left(\frac{||\Delta U^n||_\infty}{TOL} \right)^{K_P}, \tag{7}$$

$$\Delta t_{PID}^{n+1} = dt_{fac}\, \Delta t^n \left(\frac{TOL}{||\Delta U^{n+1}||_\infty} \right)^{K_I} \left(\frac{||\Delta U^n||_\infty}{TOL} \right)^{K_P} \left(\frac{TOL}{||\Delta U^{n-1}||_\infty} \right)^{K_D}, \tag{8}$$

where $dt_{fac} < 1$ is a safety factor which prevents rejected iterations.

Additionally the (so-called) predictive controller is considered in this investigation, which was designed by Gustafsson [8] for stiff equation systems. Stiff equations originate, among others, from separated space and time discretization, which is typical for the discretization of the Navier-Stokes equations. The predictive control algorithm

$$\Delta t_{PC}^{n+1} = dt_{fac}\, \Delta t^n \left(\frac{TOL}{||\Delta U^{n+1}||_\infty} \right)^{K_I} \left(\frac{||\Delta U^n||_\infty}{TOL} \right)^{K_D} \left[\frac{\Delta t^n}{\Delta t^{n-1}} \right]. \tag{9}$$

The choice of controller parameters K_I, K_P, K_D in the literature depends on the order of accuracy of the time integration scheme q and the order of accuracy of the embedded method p. Former investigations regarding ESDIRK schemes and their error estimation skills showed that for different methods the parameter choice depends not only on the order but also on the scheme itself (and test problem). Therefore the focus of this paper lies on the controller coefficients.

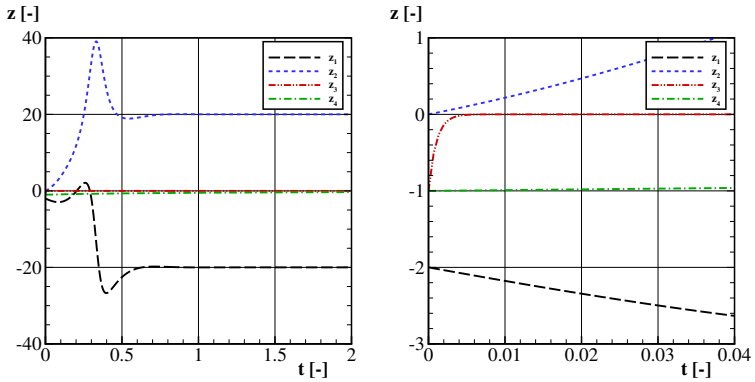

Figure 1: Analytical solution of E4 problem

Inappropriate parameter settings can lead to several controller failures: too aggressive time step adaption, alternating time step sizes, very small step sizes, decreasing step sizes with decreasing error or increasing step size with increasing error.

5 APPLICATION

5.1 Non-linear stiff ordinary differential equation system

For the basic validation of the ESDIRK error estimation the analytical test problem E4 given by Enright [9] was used, cf. [5]. The analytical solution for this system of ordinary differential equations allows an exact comparison with the numerical solution and enables a comparison of estimated and exact errors. Being non-linear and stiff, this test problem is representative of the discretized Navier-Stokes equations. The problem is given as follows

$$y = Uz, \;\; y(0) = (0, -2, -1, -1)^T \;\text{ with}$$

$$\begin{aligned} z_1' &= -(\beta_1 z_1 - \beta_2 z_2) + \tfrac{1}{2}(z_1^2 - z_2^2) \\ z_2' &= -(\beta_2 z_1 - \beta_1 z_2) + z_1 z_2 \\ z_3' &= -\beta_3 z_3 + z_3^2 \\ z_4' &= -\beta_4 z_4 + z_4^2 \end{aligned} \quad , \quad U = \tfrac{1}{2}\begin{bmatrix} -1 & 1 & 1 & 1 \\ 1 & -1 & 1 & 1 \\ 1 & 1 & -1 & 1 \\ 1 & 1 & 1 & -1 \end{bmatrix}, \quad \beta = \begin{bmatrix} 10 \\ -10 \\ 1000 \\ 0.001 \end{bmatrix}.$$

Here this test problem is used to investigate the time step control algorithms. The solution in the time interval $t = 0 - 0.2$ is shown in Figure 1 with a detailed view on the stiff starting region of component z_3. This time interval is considered throughout the whole study.

Error Estimation: A comparison of the analytical Δz_N and estimated error Δz_S obtained using $N = 100$ iterations to resolve the time period is shown in Figure 2. In order to obtain the error of a single Runge-Kutta step, each new step is initialized with the analytical solution. In general the various methods all provide a good estimate of the errors. In particular, however, the

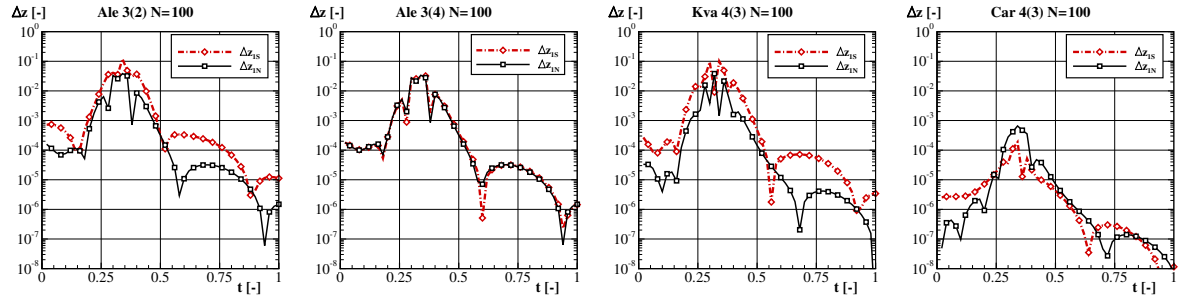

Figure 2: Error estimation Δz_S and analytical error Δz_N of component z_1 for different schemes

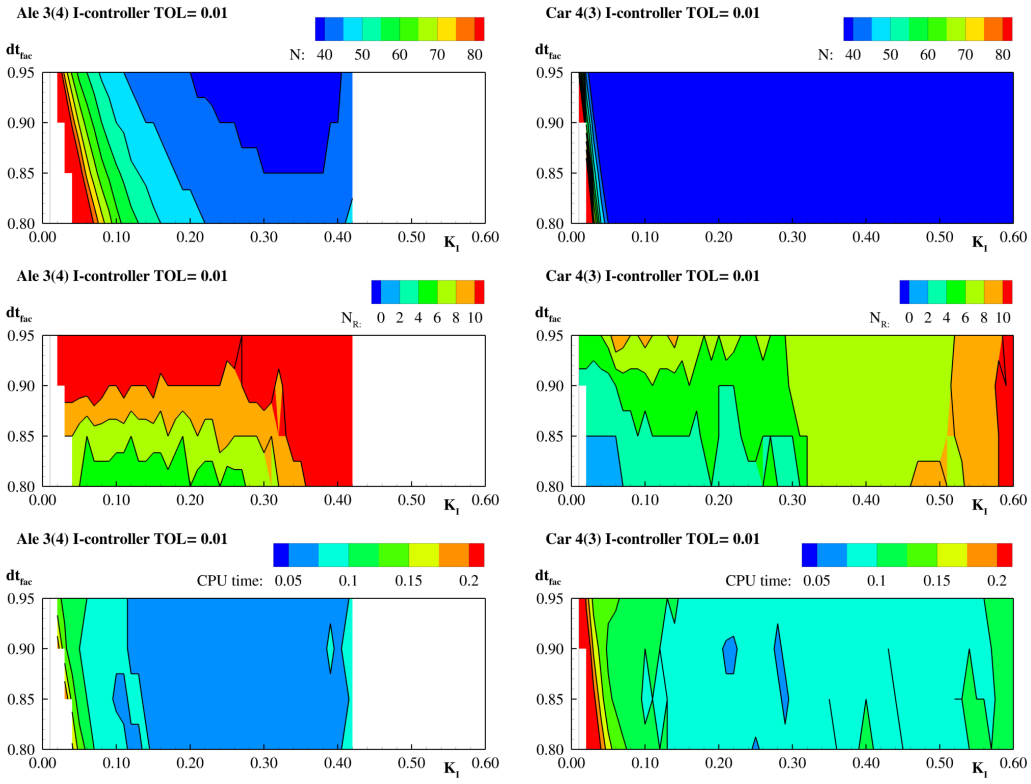

Figure 3: I-controller using Ale 3(4) (left) and Car 4(3) (right)

estimation scheme of Ale 3(4) produces the most accurate error trend and error level. In contrast Car 4(3) tends to underpredict the error. However, the error level is two orders of magnitude smaller due to the higher order of accuracy of the solution scheme.

To analyze the different controller types a systematic investigation of safety factor Δt_{fac} and parameters K_I, K_P, K_D is conducted. The influence of the safety factor was first tested using the I-Control and to reduce the effort for the following tests in consequence fixed to $dt_{fac} = 0.90$. Areas with any kind of controller failure are blanked in the figures concerning control parameter settings. Remember that this means not necessarily a total failure of the controller, also inappropriate parameters are blanked, e.g. producing long run times due to small step sizes.

I-controller: The resulting number of accepted time steps N for the integral element are given in Figure 3 for Ale 3(4) and Car 4(3), the number of rejected time steps N_R and the CPU time are also shown. Four values in the range of 0.80-0.95 are used to test the impact of dt_{fac}. The sampling of K_I in this test is much finer resolved using 60 points between $0.01 - 0.60$. Preliminary investigations showed that for most ESDIRK schemes the maximum allowable K_I is within this range. Here Ale 3(4) and Car 4(3) are shown exemplarily, which are the time integration methods with the highest sensitivity to control parameter choice, respectively lowest sensitivity. Car 4(3) is less sensitive to the parameter choice and performs over a broad parameter range very well. For all other methods the parameter range is limited. With increasing dt_{fac} the number of rejected steps slightly increases for Ale 3(4). On the other hand, together with the number of accepted steps, nearly the same number of overall iterations results. Δt_{fac} prevents for rejected time steps but is not the key factor to reduce overall number of time steps and therefore runtime.

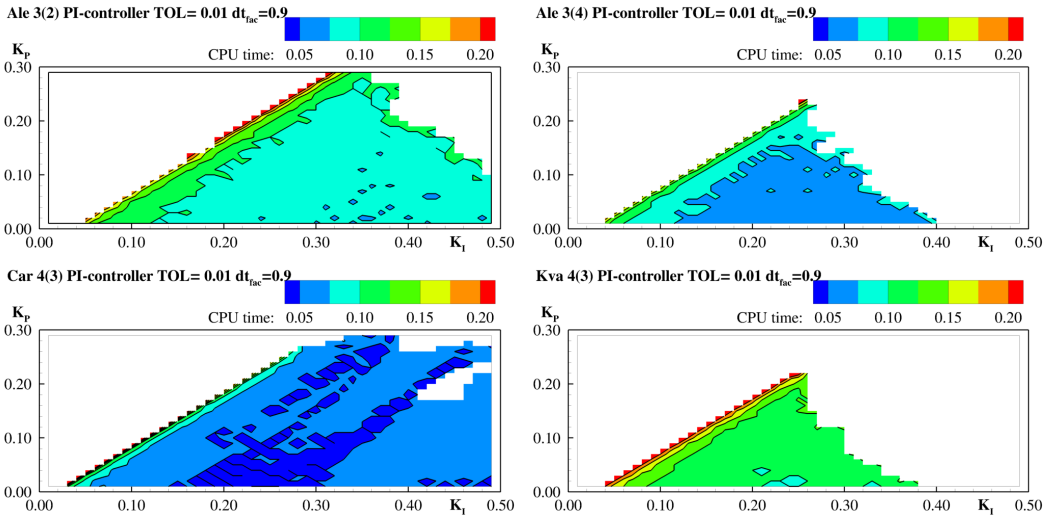

Figure 4: CPU time for PI-Control

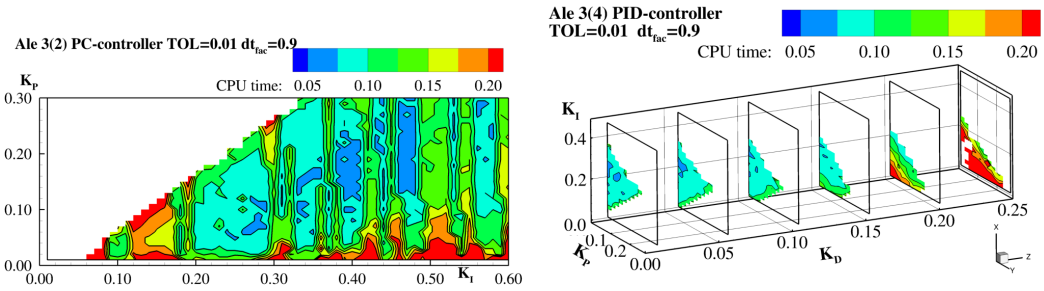

Figure 5: CPU time for Ale 3(2) using PC-Control (left) and Ale 3(4) using PID-Control (right)

PI-controller: Figure 4 compares the runtime for different ESDIRK schemes using Algorithm 7 for step size adaption. Here a fine sampling mesh with 29 points for K_I and 49 points for K_P is applied. The influence of the order of accuracy is clear lower order pairs such at Ale 3(2) tend to longer run times than methods with higher order e.g. Ale 3(4) or Car 4(3). Kva 4(3) contradicts this statement and is not well suited to this problem. Using this time step control algorithm the parameter range for Car 4(3) is nearly as limited as for the other integration schemes using this controller type. However, comparing I- and PI-Controllers it can be seen that the more sophisticated PI-Controller is able to produce lower runtimes, e.g. Car 4(3). This superiority is not that obvious for other methods.

PC-controller: Using the example of Ale 3(2) in Figure 5 (left) the time consumption for the predictive control algorithm (Equation 9) is shown. The results are scattered strongly within parameter space, small parameter changes cause large changes in runtime behaviour. Here this performance is only shown for one ESDIRK method, but it is a general result for all methods under consideration using this controller type.

PID-controller: The control parameter study for a controller of PID-type was performed using a sampling of 24 values for K_I and 14 values for K_P and K_D. In Figure 5 (right) results for Ale 3(4) are shown. With increasing values of K_D larger areas with increasing CPU time occur. An improvement of CPU time in comparison to PI-Control is not observed, however the risk of inappropriate parameter settings increases.

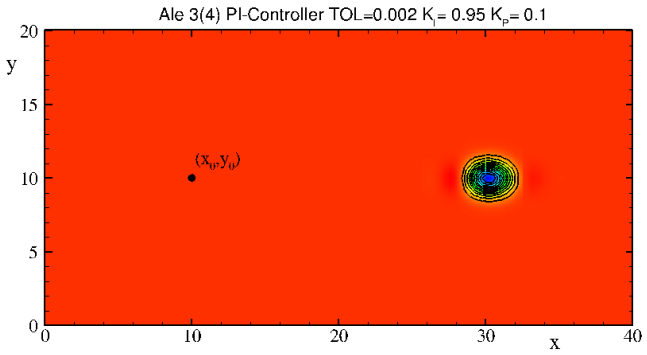

Figure 6: Computational domain and density contours at the end position

5.2 Advection of entropy disturbance

To investigate the implementation of adaptive time stepping in the context of the Navier-Stokes flow solver first a two-dimensional test problem is considered: the advection of an entropy disturbance. The simplicity of this problem facilitates a systematic controller parameter study in the Navier-Stokes solver. This is realized by initializing the density field as follows

$$\rho = \left[T_\infty - 0.001 e^{(1-r^2)}\right]^{\frac{1}{\gamma-1}}$$

with $r = \sqrt{(x-x_0)^2 + (y-y_0)^2}$ and $\gamma = 1.4$ (ratio of specific heats). The freestream values of axial velocity, pressure and temperature are $U_\infty = s135.6$ m/s, $P_\infty = 90500$ Pa and $T_\infty = 278.977$ K, respectively. The flow is uniform with $u = U_\infty$, $v = w = 0$ and $p = P_\infty$. The two-dimensional computational domain is a simple rectangle meshed with 12800 cells, split over 8 blocks, extended $40l$ in x-direction and $20l$ in y-direction, cf. Figure 6. The simulation starts at $t = 0$ with the entropy disturbance centered at $(x_0, y_0) = (10l, 10l)$ and ends about $(x_T, y_T) = (30l, 30l)$.

To analyze automatic time step adjustment and control mechanisms in the context of the flow solver a similar parameter study to that of the E4 problem with less sampling points is conducted. The prescribed tolerance of $TOL = 0.002$ is very stringent. Preliminary investigations, in which the tolerance targets were decreased from $0.01 - 0.001$, showed that this value is a threshold, which leads to strongly increased runtimes. Again the safety factor dt_{fac} is only considered for the I-controller and for all other controllers is fixed to $dt_{fac} = 0.96$.

I-controller: The resulting CPU time for all ESDIRK methods using the integral element are given in Figure 7. The number of rejected time steps N_R varies between 2 and 8, where two steps are needed to meet the prescribed tolerance in the first time step. Four values for $dt_{fac} = 0.87 - 0.96$ are studied and 10 values of $K_I = 0.05 - 0.95$. The valid parameter range is similar for all investigated time integration schemes, as well the areas with lowest and highest time consumption. A low value of dt_{fac} results in increasing CPU time, especially using Car 4(3) for time integration. In contrast to the results of E4 here the highest value of K_I yields the fastest runtime. Compared to the third-order accurate schemes, Car 4(3) does not reflect the superiority as shown for E4 problem. This scheme has six-stages while the other schemes have four or five stages. It becomes apparent that the number of stages influences the computational overhead of the flow solver. For this simple flow problem the higher order accuracy is not crucial for time consumption. In particular, with increasing number of rejected time steps (small dt_{fac}) the runtime increases dramatically.

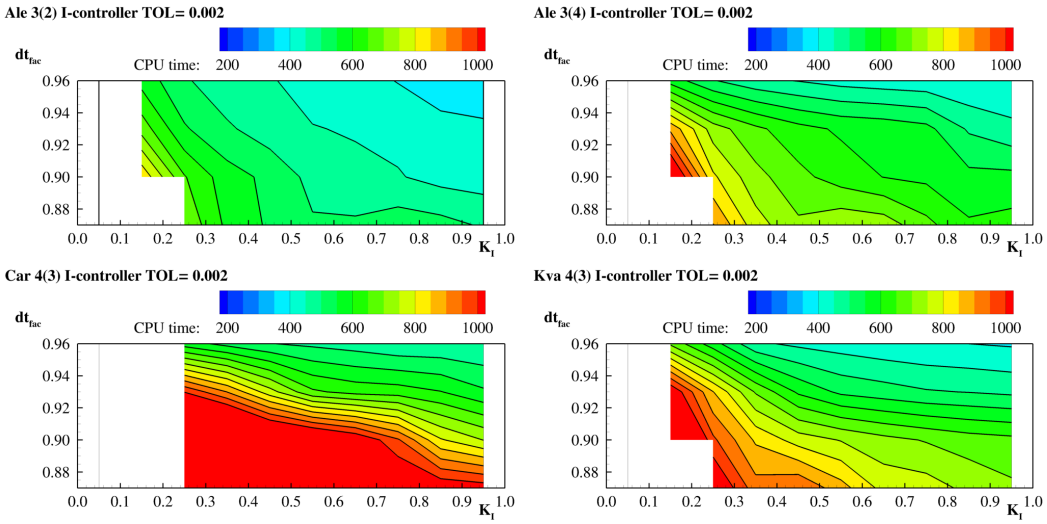

Figure 7: CPU time for advection problem using I-controller

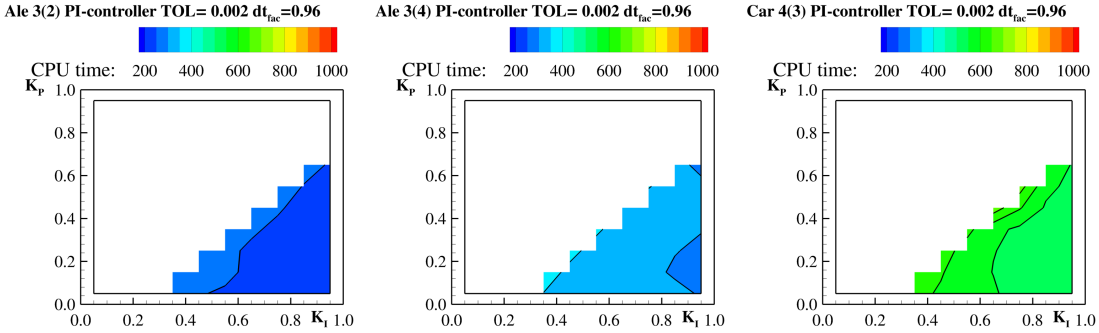

Figure 8: CPU time for advection problem using PI-Control

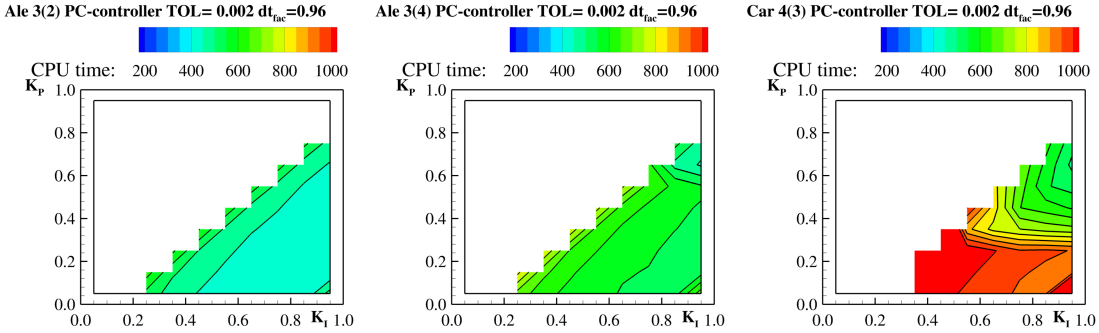

Figure 9: CPU time for advection problem using PC-Control

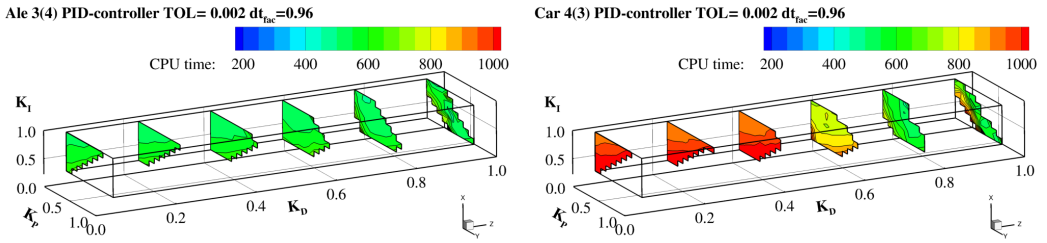

Figure 10: CPU time for advection problem using PID-Control

PI-controller: The proportional integral element is tested using 10 values for K_I and K_P in the range of $0.05 - 0.95$. The valid parameter range for PI-control is similar for all ESDIRK schemes, Figure 8. Results for Kva 4(3) are similar to Car 4(3) (not shown here). The proportional element, in addition to the integral element, smoothes the resulting runtimes over the whole parameter range. The fastest simulations are performed using high values of K_I and low values of K_P, e.g. Ale 3(4).

PC-controller: In the simulations performed using control algorithm 9 the same parameter range as for the PI type is considered, cf. Figure 9. Here longer run times are obtained. In particular, Car 4(3) shows significant higher simulation times in areas with low values of K_P. For this scheme a wide spread of the results with small parameter changes is observed, which makes it difficult to select a proper parameter combination. Kva 4(3) leads to similar CPU time to Ale 3(4) (not shown here). Although this controller type was specifically designed for stiff equation systems it does not seem to provide better results than the standard PI-controller in our investigations.

PID-controller: In Figure 10 resulting CPU times using Algorithm 8 for adaptive time stepping are shown. The parameter K_I ranges from $0.25 - 0.95$ using 8 samples and 10 samples for K_P, K_D in the range of $0.05 - 0.95$. With increasing K_D valid parameter combinations decrease. A remarkable feature of Ale 3(4) method is an almost constant CPU time for all parameter combinations. Furthermore, the region with $K_D = 0.6$ seems to be the preferred choice, due to largest area of valid combinations. In contrast, the Car 4(3) method shows a considerable decrease of simulation time with increasing K_D. Here, the region with $K_D = 0.8$ yields comparable runtime results as Ale 3(4), together with a larger region of valid combinations as for higher or lower values.

5.3 Flow around a circular cylinder

The basic investigations of controller coefficients and the implementation of embedded ESDIRK schemes in conjunction with adaptive time step control in the context of the Navier-Stokes solver were demonstrated using analytical problems. Now, as a final test case, a more realistic final problem is considered: the flow around a circular cylinder. As a further increase of complexity, the viscous effects are now captured by the two-equation k-ω turbulence modell of Wilcox [10]. The Reynolds number is 140.000, based on the cylinder diameter of 0.010137m. The free stream values for velocity and temperature are 21.20 m/s and $24°$C. The vortex shedding period is 0.02665 s, which corresponds to a Strouhal number of 0.179.

In contrast to preliminary test cases the computational effort for one simulation of the cylinder flow is much higher, therefore the number of control algorithms as well as the number of coefficients is reduced. Based on the results for the analytical problems, E4 and the advection of an entropy disturbance, here controllers of PI-type are used. For this flow problem a high value of $\Delta t_{fac} = 0.96$ is suitable.

As shown in the previous sections, the entropy advection problem, which is governed by Navier-Stokes equations, yields a region of appropriate controller parameters which is quite different than the corresponding region of the generic E4 test case, which is governed by an other differential equation system. Hence, the type of ODE system seems to have a major influence on the controller parameters. To test this assumption, another Navier-Stokes test case is investigated in this section. In other words, it is assumed that the same type of ODE system leads to the same range of suitable controller parameters. Due to the similar range of suitable K_I and K_P parameters for all methods in the previous Navier-Stokes test case, only Ale 3(4) method is investigated in this test case, and the corresponding results are considered

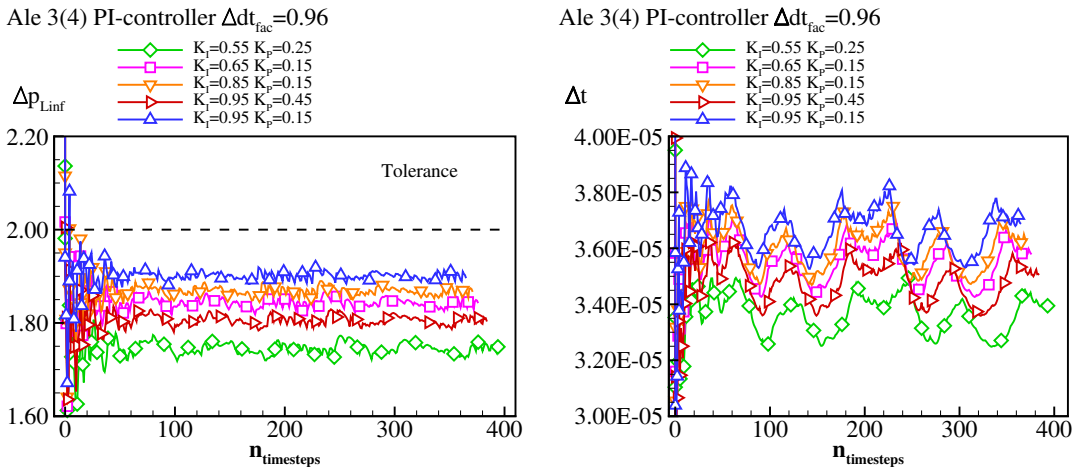

Figure 11: Cylinder flow using PI-Controller error of pressure Δp_{Linf}(right) and time step size Δt for Ale 3(4)

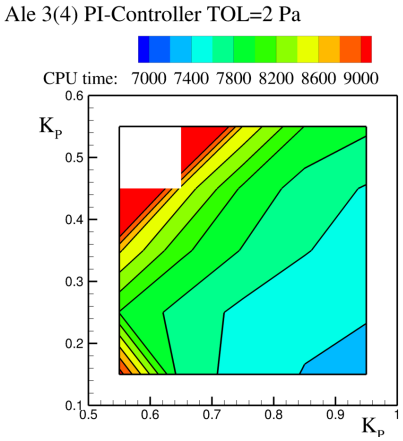

Figure 12: Cylinder flow using PI-controller for Ale 3(4)

as representative for all methods. For this problem a tolerance for the maximum pressure error of $\Delta p_{Linf} = 2\ Pa$ is prescribed.

Five simulations with different controller coefficients using Ale 3(2) are presented in Figure 11. As a beneficial result, it is found that all parameter combinations provide estimated errors, which are lower than the prescribed value. However, the simulation with small K_I and large K_P value provides a significantly smaller estimated error, making the simulation too conservative. This in turn leads to a large number of timesteps and a long simulation duration. In contrast, the combinations with large K_I and small K_P values run much closer to the prescribed tolerance, reducing the number of time steps by ca. $5\ \%$. This observation is in agreement with the time step size Δt results at the right hand side of the figure, where the largest values are found for the latter parameter combination.

Figure 12 confirms the assumption that the suitable parameters strongly depend on the governing equations. The region of valid parameter combinations, which simultaneously yields the shortest simulation duration, coincides very well with the results from the advection problem.

6 CONCLUSIONS

In this work different control algorithms for time step size control in unsteady flow simulations based on the compressible Navier-Stokes equations using embedded Runge-Kutta schemes have been investigated. Here a detailed analysis of parameter settings for time step size adaption using I-, PI-, PID- and PC-Control has been performed with the aim of calibrating the controllers for unsteady flow simulations.

Prior to the implementation in the Navier-Stokes solver a stiff analytical problem is considered to verify the precision of error prediction and for the basic understanding of different control algorithms. This test case is used for a detailed study of controller types and parameter range. In general the quality of error estimation for different ESDIRK schemes is very good. For example, the embedded ESDIRK method using the highest order scheme for error prediction, Ale 3(4), yields excellent results. However, in some cases, the estimated error is smaller than the analytical error by almost one order of magnitude.

The implementation of adaptive time step control in the flow solver is examined first with a simple advection problem, which allows for large controller parameter studies. As second test case the flow around a cylinder is used, at which only a selected number of controller coefficients is considered.

Even with the simplest controller type which contains only an integral element adaptive time stepping can be performed. The more sophisticated PC-Controller recommended by Gustafsson for stiff equations shows conflicting results, ranging from well suited for a simple advective flow problem to very poor performance for academic test problem. The PID-controller may provide region of well behaved combinations, but the resulting CPU time is much longer than for concurrent controllers. Overall, the PI-controller outperforms all other controllers for all investigated test cases. Finally, the region of suitable parameter combination depends strongly on the governing equations, which are to be solved. For the Navier-Stokes solver a high value of K_I and a low value of K_D are favourable.

REFERENCES

[1] R. Alexander. Design and implementation of DIRK integrators for stiff systems. *Applied Numerical Mathematics*, 46(1):1–17, 2003.

[2] C. A. Kennedy and M. H. Carpenter. Additive Runge-Kutta Schemes for Convection-Diffusion-Reaction Equations. *Applied Numerical Mathematics*, 44(1-2):139–181, 2003.

[3] A. Kvaerno. Singly Diagonally Implicit RungeKutta Methods with an Explicit First Stage. *BIT Numerical Mathematics*, 44:489–502, 2004.

[4] G. Ashcroft, C. Frey, K. Heitkamp, and C. Weckmüller. Advanced Numerical Methods for the Prediction of Tonal Noise in Turbomachinery - Part I: Implicit Runge-Kutta Schemes. *J. Turbomach.*, 136(2):021003–021003, 2013.

[5] K. Kozulovic and G. Ashcroft. Temporal Error Estimation and Adaptive Time Step Control in Unsteady Flow Simulations. In *WCCM XI, ECCM V, ECFD VI, July 20 - 25, 2014, Barcelona, Spain*, 2014.

[6] D. Nürnberger, F. Eulitz, and A. Zachcial. Recent Progress in the Numerical Simulation of Unsteady Viscous Multistage Turbomachinery Flow. In *15th International Symposium on Air Breathing Engines, Bangalore, India, Paper 2001-1082*, 2001.

[7] E. Kügeler. Numerical Method for the accurate analysis of cooling efficiency in film-cooled turbine-blades. Technical report, Institute of Propulsion Technology, German Aerospace Center, published in German, 2005. DLR Forschungsbericht 2005-11, Köln, 2005.

[8] K. Gustafsson. Control-theoretic techniques for stepsize selection in implicit runge-kutta methods. *ACM Trans. Math. Softw.*, 20(4):496–517, December 1994.

[9] W. H. Enright, T. E. Hull, and B. Lindberg. Comparing numerical methods for stiff systems of ODEs. *BIT Numerical Mathematics*, 15(1):10–48, 1975.

[10] David C. Wilcox. Multiscale model for turbulent flows. *AIAA Journal*, 26:1311–1320, 1988.

A BUTCHER TABLEAUS

$\gamma = 0.435866521508$

$b_1 = \frac{-18\gamma c_3+12\gamma^2 c_3+3c_3+12\gamma-12\gamma^2-2}{12\gamma c_3}$
$b_2 = \frac{2-3c_3+6\gamma c_3-6\gamma}{12\gamma(2\gamma-c_3)}$
$b_3 = \frac{6\gamma^2+1-6\gamma}{3c_3(c_3-2\gamma)}$

0	0			
2γ	γ	γ		
c_3	$\frac{6\gamma c_3-c_3^2-4\gamma^2}{4\gamma}$	$\frac{-c_3(c_3-2\gamma)}{4\gamma}$	γ	
1	b_1	b_2	b_3	γ
	b_1	b_2	b_3	γ
	$\hat{b_1}$	$\hat{b_2}$	$\hat{b_3}$	$\hat{b_4}$

Ale 3(2): $c_3 = \frac{1}{2} + \frac{\gamma}{4}$

$\hat{b_1} = b_1 - \delta b_2 - 0.096 + 0.284$
$\hat{b_2} = b_2 + \frac{-c_3 0.096+0.284}{2\gamma}$
$\hat{b_3} = b_3 + 0.096$
$\hat{b_4} = \gamma - 0.284$

Ale 3(4): $c_3 = \frac{18}{13}\gamma^2 - 2\gamma + \frac{14}{13}$

$\hat{b_1} = \frac{12\gamma c_3-4\gamma-2c_3+1}{24\gamma c_3}$
$\hat{b_2} = \frac{2c_3-1}{24\gamma(2\gamma-c_3)(2\gamma-1)}$
$\hat{b_3} = \frac{1-4\gamma}{12c_3(2\gamma-c_3)(c_3-1)}$
$\hat{b_4} = \frac{3+12\gamma c_3-4c_3-8\gamma}{12(2\gamma-1)(c_3-1)}$

Table 2: Ale 3(2) and Ale 3(4): Four-stage, 3rd-order ESDIRK method with embedded 2nd- or 4th-order scheme

$\gamma = 0.5728160625$

$a_{31} = \frac{144\gamma^5-180\gamma^4+81\gamma^3-15\gamma^2+\gamma}{(12\gamma^2-6\gamma+1)^2}$
$a_{32} = \frac{-36\gamma^4+39\gamma^3-15\gamma^2+2\gamma}{(12\gamma^2-6\gamma+1)^2)}$

0	0				
2γ	γ	γ			
$a_{31}+a_{32}+\gamma$	a_{31}	a_{32}	γ		
1	$\hat{b_1}$	$\hat{b_2}$	$\hat{b_3}$	γ	
1	b_1	b_2	b_3	b_4	γ

$\hat{b_1} = \frac{-144\gamma^5+396\gamma^4-330\gamma^3+117\gamma^2-18\gamma+1}{12\gamma^2(12\gamma^2-9\gamma+2)}$
$\hat{b_2} = \frac{72\gamma^4-126\gamma^3+69\gamma^2-15\gamma+1}{12\gamma^2(3\gamma-1)}$
$\hat{b_3} = \frac{(-6\gamma^2+6\gamma-1)(12\gamma^2-6\gamma+1)^2}{12\gamma^2(12\gamma^2-9\gamma+2)(3\gamma-1)}$

$b_1 = \frac{(288\gamma^4-312\gamma^3+120\gamma^2-18\gamma+1}{48\gamma^2(12\gamma^2-9\gamma+2)}$
$b_2 = \frac{24\gamma^2-12\gamma+1}{48\gamma^2(3\gamma-1)}$
$b_3 = \frac{-(12\gamma^2-6\gamma+1)^3}{48\gamma^2(3\gamma-1)(12\gamma^2-9\gamma+2)(6\gamma^2-6\gamma+1)}$
$b_4 = \frac{-24\gamma^3+36\gamma^2-12\gamma+1}{24\gamma^2-24\gamma+4}$

Table 3: Kva 4(3): Five-stage, 4th-order ESDIRK method with embedded 3rd-order scheme

0	0					
$\frac{1}{2}$	$\frac{1}{4}$	$\frac{1}{4}$				
$\frac{83}{250}$	$\frac{8611}{62500}$	$-\frac{1743}{31250}$	$\frac{1}{4}$			
$\frac{31}{50}$	$\frac{5012029}{34652500}$	$-\frac{654441}{2922500}$	$\frac{174375}{388108}$	$\frac{1}{4}$		
$\frac{17}{20}$	$\frac{15267082809}{155376265600}$	$-\frac{71443401}{120774400}$	$\frac{730878875}{902184768}$	$\frac{2285395}{8070912}$	$\frac{1}{4}$	
1	$\frac{82889}{524892}$	0	$\frac{15625}{83664}$	$\frac{69875}{102672}$	$-\frac{2260}{8211}$	$\frac{1}{4}$
	$\frac{82889}{524892}$	0	$\frac{15625}{83664}$	$\frac{69875}{102672}$	$-\frac{2260}{8211}$	$\frac{1}{4}$
	$\frac{4586570599}{29645900160}$	0	$\frac{178811875}{945068544}$	$\frac{814220225}{1159782912}$	$-\frac{-3700637}{11593932}$	$\frac{61727}{225920}$

Table 4: Ken 4(3): Six-stage, 4th-order ESDIRK method with embedded 3rd-order scheme